Biochimica et Biophysica Acta, 509 (1978) 111—128

BBA 78000

THE EFFECTS OF THE THERMAL PREPHASE TRANSITION AND SALTS ON THE COAGULATION AND FLOCCULATION OF PHOSPHATIDYLCHOLINE BILAYER VESICLES

NILS O. PETERSEN and SUNNEY I. CHAN *

Arthur Amos Noyes Laboratory of Chemical Physics **, *California Institute of Technology, Pasadena, Calif. 91125 (U.S.A.)*

(Received August 19th, 1977)

Summary

Absorbance measurements of sonicated dipalmitoyl phosphatidylcholine vesicles reveal two aggregation processes: flocculation and coagulation. Flocculation is only observed for samples in monovalent cationic salt solutions or in salt-free suspensions. This process is abolished in the presence of di- or trivalent cations. It is also found to be strongly temperature dependent, occurring only below the thermal prephase transition of the lipid. Dispersal of the flocculates is rapid but they re-form at a rate dictated by the hysteresis in the prephase transition. In contrast, coagulation is slow. The extent of coagulation does not seem to be strongly dependent on the temperature, the nature of the electrolyte or its concentration. The relation of the coagulated state to vesicle-vesicle fusion is briefly discussed.

Introduction

Small phospholipid bilayer vesicles tend to undergo vesicle-vesicle fusion [1—3] and are excellent systems in which to study the membrane fusion process. It is possible that appropriately prepared vesicles may be used to introduce, through vesicle fusion with the cell membrane, selected membrane components into specific cell membranes. Analogously, it is likely that chemical agents contained within the vesicle can be injected into selected cells through a fusion process. The details of how the fusion process occurs and how it may be controlled and targeted in vitro or in vivo are not yet well established. It has been shown (refs. 3 and 4, and Lee, Y.K. and Chan, S.I, unpublished) that the presence of fatty acid or lysophosphatidylcholine components

* To whom requests for reprints should be sent.
** Contribution No. 5628.

in the vesicle bilayer tends to enhance the rate of vesicle-vesicle fusion in certain cases. Similarly, surface-active agents, specifically alamethicin, have been found to accelerate the fusion process when present on the external bilayer surface [5]. The effect of these agents may be 2-fold. First, they may modify the surface properties of the bilayer so as to allow for vesicle-vesicle contact for a long enough period of time for fusion to occur. Second, they may destabilize the membrane structure such that fusion becomes more favorable. Since membrane-membrane surface contact is bound to a prerequisite for fusion it is of great importance to understand the aggregation states of the vesicles and how these states may be controlled to prevent and enhance a fusion process. In this report, we present the results of some light scattering studies designed to shed some light on this point. In particular, we will describe the effect of salt type and concentration as well as temperature on the aggregation processes in suspensions of small sonicated dipalmitoyl phosphatidylcholine vesicles.

Materials and Methods

Dipalmitoyl phosphatidylcholine was obtained from Calbiochem, Inc. and was used as received except in a few experiments where, as noted in the text, highly purified material was employed. The purification was carried out by thick-layer chromatography on silicic acid plates eluted with chloroform/methanol/water 65 : 25 : 4, (v/v).

Unsonicated lipid dispersions (liposomes) were prepared by mixing the solid lipid and the aqueous solution on a vortex mixer for several minutes while heating the sample with an air gun (sample temperature: 60—70° C). This dispersion was then diluted to the desired concentration. Sonicated lipid suspensions were prepared by subjecting a dispersion, prepared as above, to 15 min continuous sonication with a 150W MSE probe sonicator. During sonication the sample was usually immersed in a room temperature glycerol or water bath. The sample temperature reached 40° C within 45 s, 50° C after about 4 min and a final temperature of about 60° C after 15 min of sonication. At the end of the sonication, the sample was air cooled to room temperature within a few minutes and either centrifuged for 5 min at moderate speed on an Adams Safeguard centrifuge or filtered through 0.45 μm Millipore filters to remove unwanted Ti particles from the probe and small amounts of multilamellar lipid fragments. The first measurements on the samples were usually performed within 10—15 min after the sonication, except in the few cases noted otherwise in the text.

Absorbance measurements were made at λ = 450 nm using a Beckman ACTA CIII spectrophotometer equipped with a Beckman TM programmer and a Hewlett Packard 7035B XY recorder. The temperature programmer allowed for heating and cooling at constant rates. Continuous monitoring of absorbance and temperature via the XY recorder yielded the melting curves. Some melting curves were also recorded point-by-point with a Beckman DU spectrophotometer equipped with a home-made temperature programmer utilizing circulating water.

Differential thermal analysis was carried out with a Dupont 900 differential

thermal analyzer. The samples were prepared in 2-mm outside diamter capillaries by equilibrating about 5—10 mg lipid with 5—10 λ aqueous solution in the capillary at 65° C for 1—2 h.

Analysis of absorbance measurements

For a non-absorbing system which scatters light, one defines the turbidity, τ, for a 1 cm path length by

$$\tau = -\ln\left(\frac{I}{I_0}\right) = -2.303 \log\left(\frac{I}{I_0}\right) = 2.303\, A. \tag{1}$$

It is a measure of the integrated intensity of light scattered at all angles. Here I_0 is the incident intensity, I, the intensity of the transmitted light and A, the measured absorbance. Since [6,7]

$$I_0 - I = \frac{16\pi}{3} I_0 R_0 Q \tag{2}$$

the turbidity can be written as

$$\tau = -\ln\left(1 - \frac{16\pi}{3} R_0 Q\right). \tag{3}$$

R_0 is the Rayleigh ratio in the well-known Rayleight scattering limit.

$$R_0 = \frac{2\pi^2 M c \bar{n}_0^2 (\partial \bar{n}/\partial c)^2}{N\lambda^4} \tag{4}$$

and Q is the particle dissipation factor defined by the following integral of the particle scattering function $P(\theta)$

$$Q = \tfrac{3}{8} \int_0^{\pi} P(\theta)(1 + \cos^2\theta) \sin\theta \, d\theta. \tag{5}$$

The latter takes into account the interference of light scattered from different points within the particle. In expression 4, M is the molecular weight; c, the concentration (in g/cm^3) of the scattering particles; $\bar{n}_0$, the refractive index of the solvent; $\partial \bar{n}/\partial c$, the specific refractive index increment; N, Avogadro's number; and λ, the wavelength of incident light.

For small values of the turbidity, it may be approximated by

$$\tau \simeq \tfrac{16}{3}\, \pi R_0 Q \tag{6}$$

The approximation in Eqn. 6 is not, however, adequate if the absorbance (Eqn. 1) is greater than 0.1 cm^{-1}. For lipid vesicle suspensions and colloidal suspensions in general, the turbidity is usually larger than 0.2 cm^{-1}. Accordingly, the interpretation of the turbidity under these conditions is not as straightforward as was previously assumed [8]. In particular, a ratio of turbidity measurements at different temperatures or times does not necessarily represent the corresponding ratios of the R_0Q values.

It is possible, however, to obtain the quantity R_0Q from a turbidity measurement by Eqn. 3. Given two turbidities, τ_2 and τ_1, at two temperatures, the

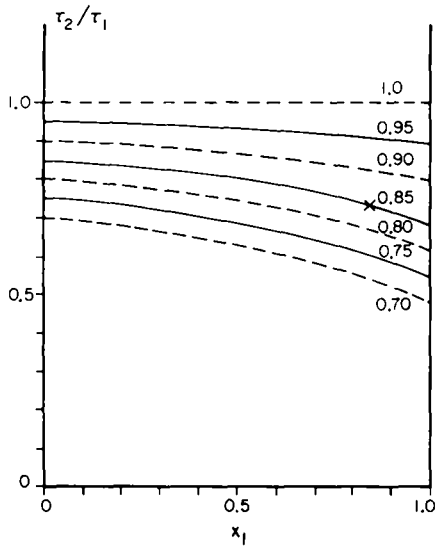

Fig. 1. The turbidity ratio τ_2/τ_1 as a function of x_1 given by Eqn. 7 for selected values of the ratio x_2/x_1 (indicated by the curves). The X illustrates that for a measured τ_2/τ_1 of 0.75 with $x_1 = 0.85$, the ratio x_2/x_1 is 0.85. These particular numbers refer to the experimental data found by Yi and MacDonald [8] (cf. Discussion).

turbidity ratio may be expressed as

$$\frac{\tau_2}{\tau_1} = \frac{x_2}{x_1}\{1 + \tfrac{1}{2}(x_2 - x_1) + \tfrac{1}{12}(4x_2^2 - x_1^2 - 3x_2x_1) + \tfrac{1}{12}(6x_2^3 - 4x_2^2x_1 - x_2x_1^2 - x_1^3) + \ldots\} \quad (7)$$

where $x_i = 16\pi R_{0i}Q_i/3$. If the turbidities are close, then the error in the approximation

$$\frac{\tau_2}{\tau_1} = \frac{x_2}{x_1} = \frac{R_{02}Q_2}{R_{01}Q_1} \quad (8)$$

is small. Fig. 1 illustrates the calculated value of the turbidity ratio τ_2/τ_1 as a function of x_1 for a series of x_2/x_1 values. The difference between the ratios is the correction from the higher order terms in Eqn. 7, which, for a typical absorbance measurement of about 0.5 cm^{-1}, amounts to about 10—20%.

Results

In the following experiments, the absorbance, A, was measured as a function of temperature and time for a series of preparations of lipids in different salt solutions. These measurements were partly prompted by the findings [8] that light scattering and turbidity measurements are indeed sensitive to phase transitions in dipalmitoyl phosphatidylcholine vesicles in salt-free solutions, and partly by the desire to explore the aggregation properties of bilayer vesicles under various conditions. In our studies we have measured the melting curves for liposomes and vesicles in $Ca(NO_3)_2$ and for vesicles in $La(NO_3)_3$, $NaNO_3$ and

salt-free solutions. We have found evidence for a pretransition in these systems and have studied the hysteresis of this transition. The time dependence of the absorbance was also monitored for vesicles. These data have provided insights into the aggregation states of the vesicles as a function of salt and temperature.

Melting curves

(i) Multilayers. The absorbance of a dilute liposome suspension (0.06% by weight dipalmitoyl phosphatidylcholine) in 40 mM $Ca(NO_3)_2$ is shown in Fig. 2 as a function of temperature. The heating curve (curve a) exhibits two abrupt decreases in absorbance, the larger of which occurs at 44° C and the smaller at about 37° C. The cooling curve (curve b) shows the change associated with the thermal phase transition at 44° C in the dipalmitoyl phosphatidylcholine bilayer but the absence of an absorbance change at the pretransition temperature is apparent. The presence of Ca^{2+} causes the phase transition temperature to be a few degrees higher [9—11] than the 41—42° C usually observed.

Numerous attempts to measure the melting curve for dilute salt-free, unsonicated lipid dispersions failed because of instability of the suspension. There was a large drift in the turbidity while the suspension settled.

In order to describe the absorbance transition curves quantitatively, it is convenient to define the following ratios

$$R_{\text{main}} \equiv \tau(T_c + \Delta T)/\tau(T_c - \Delta T)$$

$$R_{\text{pre}} \equiv \tau(T_p + \Delta T)/\tau(T_p - \Delta T) \text{ and}$$

$$R_{\text{total}} \equiv \tau(T_c + 10°\text{C})/\tau(T_c - 10°\text{C}) \qquad (9)$$

where T_c and T_p are the temperatures at which the Chapman and the pretransition, respectively, take place. ΔT is a small increment of temperature greater than the transition width. In practice, R_{main} or R_{pre} is obtained as the ratio (τ_2/τ_1) where τ_2 and τ_1 are the extrapolated values of the turbidity at T_c (or T_p) (Fig. 2, inset). The values obtained for these quantities from the data given in Fig. 2 are listed in Table I.

(ii) Sonicated vesicles in $Ca(NO_3)_2$. The equivalent melting curve for a week old, sonicated suspension of small dipalmitoyl phosphatidylcholine vesicles in 40 mM $Ca(NO_3)_2$ is also included in Fig. 2 (curve c). In this curve the transition occurs over a slightly broader temperature range and the change in absorbance through the transition is proportionally larger. It is evident from Table I that the R_{main} and R_{total} values are significantly smaller for the vesicle system, whereas R_{pre} is not much different.

(iii) Sonicated vesicles in $La(NO_3)_3$. Preparations of sonicated dipalmitoyl phosphatidylcholine vesicles in 20 mM $La(NO_3)_3$ solutions exhibit absorbance changes with temperatures which are comparable to those of vesicles in 40 mM $Ca(NO_3)_2$. There is, however, no detectable absorbance change at the pretransition temperature for these samples in $La(NO_3)_3$.

(iv) Sonicated vesicles in Neat ^2H_2O. Fig. 3 shows the heating (a, b) and cooling (a′, b′) curves for sonicated dipalmitoyl phosphatidylcholine vesicles in ^2H_2O immediately (10 min) after preparation (a, a′) and 48 h later (b, b′). The R_{main}, R_{pre}, and R_{total} values for the two heating curves are also listed in Table I. It is evident that R_{pre} and R_{total} are much smaller than those for the

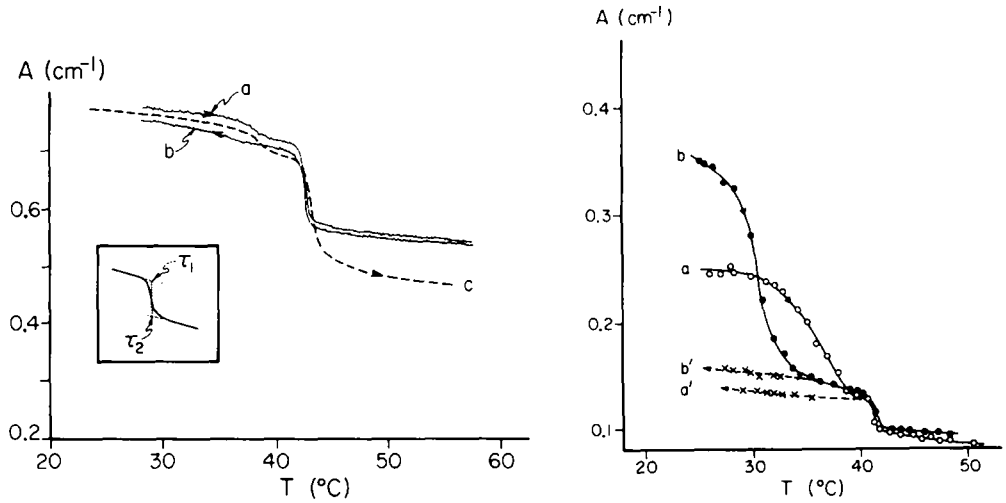

Fig. 2. Traces of the absorbance changes with temperature for a, heating of 0.06% by weight dipalmitoyl phosphatidylcholine liposomes in 40 mM $Ca(NO_3)_2$; b, cooling in the sample heated in a; c, heating of 2% by weight dipalmitoyl phosphatidylcholine vesicles in 40 mM $Ca(NO_3)_2$. The inset illustrates how the extrapolated turbidities at the transition are obtained. The ratio of τ_2 to τ_1 is used to determine R (see Eqn 9).

Fig. 3. Absorbance changes as a function of temperature for 2% by weight diplamitoyl phosphatidylcholine vesicles in ^2H_2O. a and b are heating curves, a' and b' the corresponding cooling curves. a and a' were obtained 10 min after preparation whereas b and b' were measured 48 h later for the sample kept in the meantime at room temperature.

sonicated vesicles in $Ca(NO_3)_2$ whereas R_{main} is about the same. The cooling curves once again show no absorbance changes at the pretransition. This was characteristic of all the cooling curves measured, independent of the nature of the sample. However, the absorbance change could be observed upon reheating under certain conditions.

The hysteresis of the pretransition

The cooling curves of Figs. 2 and 3 suggest that there is a hysteresis in the pretransition. It is possible to maintain the sample temperature at 28°C or

TABLE I

OBSERVED TURBIDITY RATIOS FOR SEVERAL PREPARATIONS OF PHOSPHOLIPID SUSPENSIONS

See Eqn. 9 of text for definitions of turbidity ratios.

Sample	R_{main}	R_{pre}	R_{total}
Unsonicated dimyristoyl phosphatidylcholine liposomes in $Ca(NO_3)_2$	0.89	—	—
Unsonicated dipalmitoyl phosphatidylcholine liposomes in $Ca(NO_3)_2$	0.82	0.97	0.70
Unsonicated distearoyl phosphatidylcholine liposomes in $Ca(NO_3)_2$	0.73	—	—
Sonicated dipalmitoyl phosphatidylcholine vesicles in $Ca(NO_3)_2$	0.72	0.96	0.63
Sonicated dipalmitoyl phosphatidylcholine vesicles in $La(NO_3)_2$	0.72	1.00	0.70
Sonicated dipalmitoyl phosphatidylcholine vesicles in ^2H_2O (t = 0)	0.76	0.52	0.36
Sonicated dipalmitoyl phosphatidylcholine vesicles in ^2H_2O (t = 48 h)	0.75	0.37	0.27

higher for several hours without observing any increase in the sample absorbance. However, if the temperature is maintained at 25° C, the absorbance increases slowly and reaches 50, 75 and 100% of its original value in about 10, 20 and 60 min, respectively. After 60 min the absorbance continues to increase but at a slower rate. At lower temperatures the absorbance reaches its original value faster.

The hysteresis effect of the prephase transition and the time course of recovery of sample absorbance can be correlated with a similar hysteresis observed in differential thermal analysis for the pretransition in liposomal preparations. The latter hysteresis is characterized by the observation that, following a heating and cooling cycle, the pretransition will not reappear in the subsequent differential thermal analysis heating curve unless the sample has been cooled to a temperature lower than about 8–10° C below the pretransition temperature. Furthermore, at 10–12° C below the pretransition temperature, the differential thermal analysis pretransition reappears at a slow rate and recovers fully after about an hour. At lower temperatures the recovery is substantially faster.

Qualitatively, the differential thermal analysis hysteresis effects observed in pure lipid systems and ideally mixed lipid systems are identical. A particularly well documented example of the hysteresis and the recovery is illustrated in Fig. 4 for 1 : 1 mixture of dipalmitoyl phosphatidylcholine and diperdeuteropalmitoyl phosphatidylcholine. In the sequence of thermograms b–h the

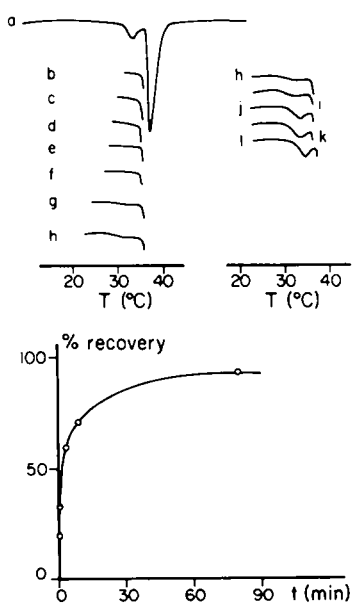

Fig. 4. Illustration of the pretransition hysteresis. (A) The sequence of differential thermal analysis heating curves labelled b to h, illustrates that there is no evidence for recurrence of the pretransition till the sample is cooled to approx. 10° C below the pretransition temperature. Lowest temperature to which the sample is cooled in these experiments is (b) 31° C, (c) 30° C, (d) 29° C, (3) 28° C, (f) 27° C, (g) 25° C, and (h) 23° C. The sequence from h to l illustrates the time rate of recovery of the pretransition when the sample is kept at 23° C for (h) 1 min, (i) 2 min (j) 5 min, (k) 10 min and (l) 80 min. (B) The recovery curve for the prephase transition when the sample is kept at 23° C.

sample is cooled to different temperatures below the pretransition and, after 1 min, is reheated. In the sequence h—l, the sample is cooled to 23° C and left from 1 to 90 min at that temperature (±1° C). The percentage recovery of the pretransition as a function of time kept at 23° C was calculated from the peak height of the thermograms labelled h—l relative to that of a. Since the main transition did not change significantly in these runs, the pretransition signal height was normalized to the main transition signal height. These results are summarized in Fig. 4.

Fig. 4 illustrates that when a liposome sample is heated through the transition and cooled to 23° C, the intensity of the differential thermal analysis pretransition on subsequent heating increases with the length of time the sample is kept at 23° C. However, the intensity never exceeds that observed in the first differential thermal analysis heating curve for samples prepared well in advance of the measurement. Similarly, when a liposome sample is heated and cooled to about 23° C, the absorbance of the sample at 23° C slowly increases and reaches but seldom exceeds the absorbance value observed for the sample at 23° C prior to the heating-cooling cycle. In contrast, the absorbance at 23° C for a vesicle sample which has been subjected to a similar heating-cooling cycle increases steadily. These latter observations will be presented in detail in the following.

Time-dependent absorbance changes for vesicle suspensions

(i) Dipalmitoyl phosphatidylcholine vesicles in Neat ^2H_2O. The effect on the heating curve of keeping a suspension of small dipalmitoyl phosphatidylcholine vesicles in ^2H_2O at 23° C for 48 h is seen in Fig. 3. At each temperature, the absorbance increases with time but to varying extents. We have followed the absorbance changes at several temperatures by measuring the entire heating curve at selected times. In order to characterize these absorbance changes we define the ratio of the turbidity at time zero to that at time t for a given temperature, T, by

$$r_T(t) = \tau(0)/\tau(t) \tag{10}$$

For the data in Fig. 3 we find $r_{25} = 0.69$ and $r_{50} = 0.95$ after the samples has been kept 48 h at room temperature. Clearly, the absorbance change over this period of time is much larger at 25° C than at 50° C. This behavior is characteristic of the absorbance for vesicles in salt-free solutions or in monovalent salt solutions (see below).

(ii) Dipalmitoyl phosphatidylcholine vesicles in monovalent salts. Samples prepared with $NaNO_3$ or NaCl exhibit absorbance changes similar to those observed for samples without salts. Because the absorbance in these systems is usually rather large and difficult to quantify, very few heating curves were actually recorded.

Vesicles prepared in neat ^2H_2O exhibit an absorbance increase when a monovalent salt solution is added at room temperature. Moreover, the increase is greater the higher the salt concentration. However, if the samples are heated to a temperature above the transition temperature, the salt-dependent absorbance increase almost disappears. The "salting-out" phenomenon is even more pronounced for vesicles prepared with purified dipalmitoyl phosphatidylcholine. In these systems, a turbid flocculate actually separates at room temper-

ature a few hours after addition of NaCl. The flocculate disperses spontaneously (without shaking or stirring) at temperatures above about 40° C, but when cooled to room temperature, the flocculate reappears within several minutes. This dispersion-flocculation cycle was observed while heating and cooling the sample for several weeks.

(iii) Dipalmitoyl phosphatidylcholine vesicles in $Ca(NO_3)_2$. When the heating curve is measured at selected times over a 200 h period for a sample of dipalmitoyl phosphatidylcholine vesicles sonicated in 40 mM $Ca(NO_3)_2$ kept at 23° C, R_{main}, R_{pre} and R_{total} remain constant while r_{25} and r_{50} decrease steadily (Fig. 5). Both r_{25} and r_{50} decrease at the same rate indicating that the phenomena responsible for the absorbance increases are not sensitive to temperature, in contrast to dipalmitoyl phosphatidylcholine in neat ^2H_2O.

We repeated the above experiments for several solutions with 1, 2 and 5% by weight dipalmitoyl phosphatidylcholine. As illustrated in Fig. 5, there appears to be no concentration dependence of the relative absorbance changes, r_{25} and r_{50}. Nevertheless, the early part of the absorbance change is compatible with

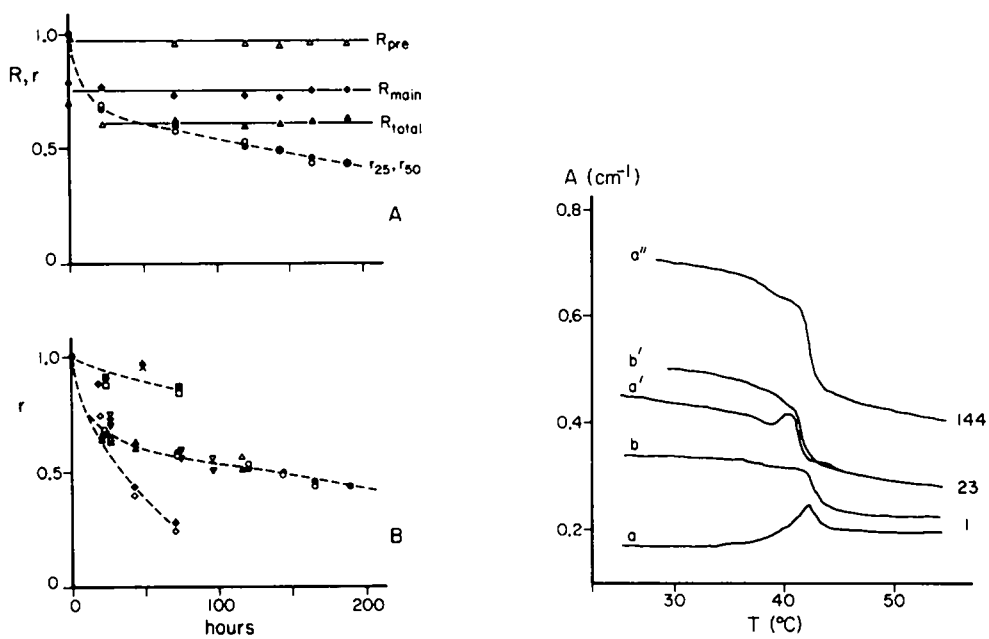

Fig. 5. (A) Time dependence of the turbidity ratios defined in Eqns. 9 and 10 for 2% by weight dipalmitoyl phosphatidylcholine vesicles. (B) r_{25} (filled symbols and x) and r_{50} (open symbols and +) defined in Eqn. 10 for various samples of dipalmitoyl phosphatidylcholine in 40 mM $Ca(NO_3)_2$. ▽, ▼, 1% by weight vesicles; ○, ●, 2% by weight vesicles; △, ▲, 5% by weight vesicles; □, ■, 1% by weight vesicles cooled slowly after sonication; ◇, ◆, 2% by weight vesicles kept at 55° C between melting curve measurements; +, X, 0.06% by weight liposomes. The samples were kept at 23° C between the melting curve measurements except for the one case noted (◇, ◆).

Fig. 6. Selected absorbance melting curves for a sample of 2% by weight dipalmitoyl phosphatidylcholine vesicles in 40 mM $Ca(NO_3)_2$ kept for 1, 23 and 144 h. Curves a, a′ and a″ are the first heating curves obtained at the time indicated whereas curves b and b′ are the heating curves obtained immediately after cooling again.

second-order aggregation kinetics and suggests

$$A + A \rightarrow A_2 \tag{11}$$

provided the absorbance increments are linearly proportional to the concentration of A_2. To elucidate the kinetics, it is necessary to extend these studies to a greater concentration range and to obtain more accurate light scattering data with better time resolution.

(iv) Dipalmitoyl phosphatidylcholine liposomes. In contrast to the steady absorbance increases observed for vesicles, the time-dependent absorbance changes for liposomes in $Ca(NO_3)_2$ are very small (Fig. 5B). Liposome suspensions exhibit large time-dependent absorbance changes. However, these effects arise from particle settling, as these suspensions are not at buoyant equilibrium initially.

Time-dependent changes in the shape of vesicle melting curves

Fig. 6 shows selected melting curves measured at various intervals after sonication for one sample of dipalmitoyl phosphatidylcholine in 40 mM $Ca(NO_3)_2$. The first heating curve (a) measured shortly after preparation exhibits a sharp rise in absorbance just below the main transition temperature (compare Fig. 2). Upon immediate cooling and reheating the melting curve assumes the shape of b, which it maintains on subsequent heating-cooling cycles. If the sample is kept at room temperature for about a day, a′ is observed in the first heating curve only. However, when it is allowed to sit another day or more at room temperature the first heating curves are always shaped like a″.

The exact shape of the melting curves in similar experiments depends on the sample preparation, but curve a in Fig. 6 is representative of dipalmitoyl phosphatidylcholine vesicles in $Ca(NO_3)_2$ or $La(NO_3)_3$. On occasion similar effects are seen in salt-free solutions.

Discussion

Origin of absorbance changes at the main transition

Yi and MacDonald [8] measured the refractive index, $\overline{n}$, and the refractive index increment, $\partial\overline{n}/\partial c$, for dipalmitoyl phosphatidylcholine dispersions as a function of temperature and found that both quantities decreased significiantly at the thermal transition of the lipid bilayer. They demonstrated that the refractive index change, and the corresponding change in $\partial\overline{n}/\partial c$, were quantitatively * accounted for by a partial molar volume change, $\Delta\overline{V}$, of the lipid. Their measured ratio of $\partial\overline{n}/\partial c$ at 42°C to that at 40°C of 0.934 yields (Eqn. 4) the ratio of R_0 values at these temperatures:

$$\frac{R_0(42°C)}{R_0(40°C)} = 0.934)^2 = 0.872 \tag{12}$$

If the particle scattering function $P(\theta)$ is unity (Rayleigh scattering limit) or if

* Yi and MacDonald [8] used a $\Delta\overline{V}$ of 1.4% to account for a 4.8% change in $\partial\overline{n}/\partial c$. More recent dilatometry data suggest a $\Delta\overline{V}$ of approx. 2.3%, which when used in their model, accounts fully for the 6.6% change in $\partial\overline{n}/\partial c$ actually observed between 40 and 42°C in their measurements.

there is no difference between the particle scattering functions at the two temperatures, then the intensity ratio of light scattered at any angle should also be 0.872. However, Yi and MacDonald [8] measured the intensity ratio at a 90° scattering angle and obtained the value of 0.75. Accordingly they argued that ratio of the particle scattering functions at the two temperatures is

$$P(90)_{42°C}/P(90)_{40°C} = 0.860 \tag{13}$$

These workers also demonstrated that the decrease in the particle scattering function upon melting was not a result of the vesicle size change, but rather due to a reduction in polarizability anisotropy. The effect of an anisotropic polarizability of the hydrocarbon chain on the particle scattering function for small vesicles was first estimated by Tinker [12], who showed that the particle scattering function at 90° is

$$P(90) = \frac{k}{15}(6\alpha_z^2 - 2\alpha_{xy}\alpha_z + 11\alpha_{xy}^2) \tag{14}$$

where k is a proportionality constant; and α_z and α_{xy} are the polarizabilities of a methylene segment along and perpendicular to the average direction of the hydrocarbon chain, namely the director.

We now show that a ratio of about 0.86 in Eqn. 13 is, in fact, to be expected from the motional state of the vesicle bilayer recently inferred from nuclear magnetic resonance experiments by Petersen and Chan [13]. To demonstrate this, we calculate the particle scattering function according to Eqn. 14 for the bilayer at temperatures below and above the transition temperature and evaluate the ratio

$$\frac{P(90)_{42°C}}{P(90)_{40°C}} = \frac{(6\alpha_z^2 - 2\alpha_{xy}\alpha_z + 11\alpha_{xy}^2)_{42°C}}{(6\alpha_z^2 - 2\alpha_{xy}\alpha_z + 11\alpha_{xy}^2)_{40°C}} \tag{15}$$

For the bilayer at 40° C we assume that the hydrocarbon chain is normal to the bilayer surface and in an *all-trans* conformation. In this case, α_z and α_{xy}, respectively, are given by the molecular polarizabilities $\alpha_{/\!/}$ and $\alpha_\perp$ of a methylene group parallel and perpendicular to the normal to the plane spanned by the CH_2 group. Numerical values for $\alpha_{/\!/}$ and $\alpha_\perp$ have been calculated, assuming the methylene group to be a cylindrically symmetric scattering element, by Ohki and Fukuda [14] to be

$$\alpha_{\parallel} = 5.72 \cdot 10^{-24}\ \text{cm}^3$$
$$\alpha_\perp = 2.96 \cdot 10^{-24}\ \text{cm}^3 \tag{16}$$

Accordingly, the denominator of Eqn. 15 is

$$(6\alpha_{\parallel}^2 - 2\alpha_\perp\alpha_{\parallel} + 11\alpha_\perp^2) = 258.83 \cdot 10^{-48}\ \text{cm}^6 \tag{17}$$

At temperatures above the phase transition temperature, we assume the motional state proposed by Petersen and Chan [13]; that is the hydrocarbon chain undergoes rapid isomerization through kink diffusion as well as much slower reorientation about a director normal to the bilayer. As a result of rapid isomerization of the chain, the effective polarizabilities parallel and perpendic-

ular to the instantaneous chain direction are [8,13]

$$\alpha'_z = \alpha_{\parallel} p_t + (\tfrac{1}{4}\alpha_{\parallel} + \tfrac{3}{4}\alpha_{\perp}) p_g$$

$$\alpha_{x'y'} = \alpha_{\perp} p_t + \tfrac{1}{2}(\tfrac{3}{4}\alpha_{\parallel} + \tfrac{3}{4}\alpha_{\perp}) p_g, \tag{18}$$

where p_t and p_g give the probabilities of a methylene segment being in a trans or *gauche* conformation, respectively. For a major portion of the chain $p_t \geqslant 0.8$ [13], thus

$$5.31 \leqslant \alpha_{z'} \cdot 10^{24}\ \mathrm{cm}^{-3} \leqslant 5.72$$

$$3.17 \geqslant \alpha_{x'y'} \cdot 10^{24}\ \mathrm{cm}^{-3} \geqslant 2.96 \tag{19}$$

In the absence of motions other than chain isomerization, then, we would have $\alpha_z = \alpha_{z'}$, $\alpha_{xy} = \alpha_{x'y'}$ so

$$(6\alpha_{z'} - 2\alpha_{x'y'}\alpha_{z'} + 11\alpha^2_{x'y'}) \geqslant 246.15 \cdot 10^{-48}\ \mathrm{cm}^6 \tag{20}$$

and a $P(90)_{42°C}/P(90)_{40°C}$ greater than 0.95, which is clearly too high in comparison with the experimental value (Eqn. 13). However, if the chains reorient about the bilayer normal then we have

$$\alpha_z = \alpha_{x'y'} + (\alpha_{z'} - \alpha_{x'y'}) \langle \cos^2 \psi \rangle$$

$$\alpha_{xy} = \tfrac{1}{2}((\alpha_{x'y'} + \alpha_{z'}) - (\alpha_{z'} - \alpha_{x'y'}) \langle \cos^2 \psi \rangle), \tag{21}$$

where ψ if the instantaneous angle of deflection of the chain relative to the director and the triangular brackets are used to denote the ensemble average over the distribution of angles $g(\psi)$. If in the motional model we assume a constant distribution in chain fluctuation within the range $0 \leqslant \psi \leqslant \Delta\psi$, then the nuclear magnetic resonance order parameter measurements suggest $\Delta\psi \geqslant 60°$ for vesicles [13]. In this limit, the particle scattering function is not very sensitive to the exact value of $\Delta\psi$ and we find

$$226.2 \leqslant (6\alpha_z^2 - 2\alpha_{xy}\alpha_z + 11\alpha^2_{xy}) \times 10^{48}\ \mathrm{cm}^{-6} \leqslant 229.0 \tag{22}$$

and

$$0.87 \leqslant P(90)_{42°C}/P(90)_{40°C} \leqslant 0.89, \tag{23}$$

a result which is in reasonable agreement with the experimentally observed ratio.

Yi and MacDonald [8] also claimed their measured turbidity ratio of 0.75 reflected the intensity, and therefore the particle scattering function ratio. The correspondence between the experimental ratios is, however, purely coincidental. Their absorbance at 42°C gives an x_1 value of 0.84 and from Eqn. 8 and Fig. 1, we predict

$$\frac{R_0(42°C)\, Q_{42°C}}{R_0(40°C)\, Q_{40°C}} = 0.85 \tag{24}$$

and hence a particle dissipation factor ratio of

$$Q_{42°C}/Q_{40°C} = 0.97 \tag{25}$$

since by Eqn. 12, $R_0(42°C)/R_0(40°C) = 0.872$. Thus, the particle dissipation factor is not very sensitive to changes in anisotropy in the effective polarizability of the hydrocarbon chains.

Pecora and Aragón [15] have generalized the calculation of the particle scattering function for vesicles composed of anisotropic chains. The multilamellar structure of a liposome may be approximated by a large vesicle with a thick bilayer. In this limit, Pecora and Aragón's results predict that there is a negligible contribution to the particle scattering function from the anisotropy of the polarizability. Consequently, the particle dissipation factor for liposome suspensions should be insentitive to changes in the polarizability anisotropy upon melting.

The turbidity ratio, R_{main}, for unsonicated dispersions in 40 mM $Ca(NO_3)_2$ is 0.82 when measured at an absorbance of 0.7. From Eqn. 8 and Fig. 1 we then obtain

$$\frac{R_0(42°C)\,Q_{42°C}}{R_0(40°C)\,Q_{40°C}} = 0.89 \tag{26}$$

But we expect $Q_{42°C}/Q_{40°C}$ to approach unity for the liposome, so that the turbidity ratio measures only the volume change associated with the transition. The different turbidity ratios for liposome preparations of dimyristoyl (DMPC), dipalmitoyl (DPPC) and distearoylphosphatidylcholine (DSPC) (Table I) therefore suggest that the volume change associated with the thermal transition in $Ca(NO_3)_2$ solutions follows the relation

$$\Delta\bar{V}_{DSPC} > \Delta\bar{V}_{DPPC} > \Delta\bar{V}_{DMPC}$$

If all turbidity changes observed with liposomal samples indeed are only due to density changes, the measurable R_{pre} suggest that there is a small change in $\Delta\bar{V}$ of the bilayer, presumably by uptake of water, at the pretransition.

The pretransition in bilayer vesicles

Most heating curves show a decrease in absorbance at a temperature near the pretransition temperature. For vesicles prepared in $Ca(NO_3)_2$, the change is quite small ($R_{pre} \approx 0.96$) and comparable to the change observed in the liposome system ($R_{pre} = 0.97$) (Figs. 2 and 3). It is likely that this absorbance decrease corresponds to the small partial molar volume increase associated with the pretransition [1]. Independent of its origin, the absorbance change along with the time course of its hysteresis provides strong evidence that vesicle bilayers undergo a transition comparable to the pretransition observed with differential thermal analysis techniques for liposomes.

The absorbance changes observed at the pretransition temperature in heating curves for vesicles in salt-free solutions are much greater than those seen for vesicles or liposomes in $Ca(NO_3)_2$. This turbidity change is due in part to a partial molar volume change of the vesicle. However, the observed time dependence of the absorbance at a given temperature could only be accounted for by an aggregation phenomenon.

States of aggregation of vesicle suspensions

Yi and MacDonald [8] and Chong and Colbow [17] observed large temper-

ature-reversible absorbance changes at the pretransition and attributed these to a cooperative aggregation-dispersion process. The latter workers only discussed the dispersion, which they described as irreversible, since they did not consider the hysteresis effects in the pretransition. The time-dependent absorbance changes observed here support the proposal that aggregation plays an important role in the vesicle system.

Since vesicles typically are 200—500 Å in diameter, they form a lyophobic colloid. Interactions among particles in a colloid have been studied extensively; in fact, a general theory has emerged from these studies [18]. Examples of the results obtained from two equally large spherical particles are illustrated in Fig. 7, where the total energy of interaction (in units of kT) is presented in terms of the center-to-center separation, R, expressed in units of the particle radius, a. The major features to note about the curves in Fig. 7 are: (i) a deep minimum (the primary minimum) in the energy for interactions at small separations, (ii) an energy barrier with a maximum at intermediate separations, (iii) a shallow minimum (the secondary minimum) in the interaction energy at nearest surface-to-surface separations comparable to the particle radius. The exact positions and magnitudes of these extrema depend on the particle size and surface charge and the electrolyte composition and concentration *.

Theoretical calculations of curves similar to those shown in Fig. 7 have been performed assuming different surface potentials for the particle and using different electrolyte concentrations and charges [18,19]. These calculations suggest the following trends: (i) if the surface potential of the particle is increased, the maximum rises and the secondary minimum becomes less pronounced. (ii) If either the electrolyte concentration or charge is decreased, the Debye length of the Gouy-Chapman double layer increases. Qualitatively, this produces the same effects on the curves as an increased surface potential. (iii) The position and depth of the primary minimum is rather insensitive to changes in surface properties or electrolyte composition. (iv) The secondary minimum is quite shallow except in cases where the maximum approaches kT and the particle radius is about 10^{-6}—10^{-5} cm.

These theoretical results indicate that intervesicular interactions may result in both close, practically irreversible contacts and distant, loose associations. We adopt the terms coagulation and flocculation, respectively [20], to describe the processes leading to these states, and propose that a colloidal suspension of vesicles may exist in any of the states illustrated in Fig. 8: isolated, coagulated, flocculated, aggregated and fused. The time-dependent absorbance changes reported here, we surmise, reflect transformations among these various states.

Isolated vesicles are probably only found in dilute samples just after sonication. It should be possible to favor the isolated state by increasing the vesicle surface potential or decreasing the ionic strength. Indeed, vesicles with fatty acid impurities [3,4] or in low salt solutions are stabilized.

Flocculates of vesicles are formed through the long-range interactions

---

* More recent calculations accounting for both retarding and many-body effects confirmed the qualitative features of the curves in Fig. 7, although the numerical details differ slightly (Nir, S. (1977) Prog. Surf. Sci. 9, 1).

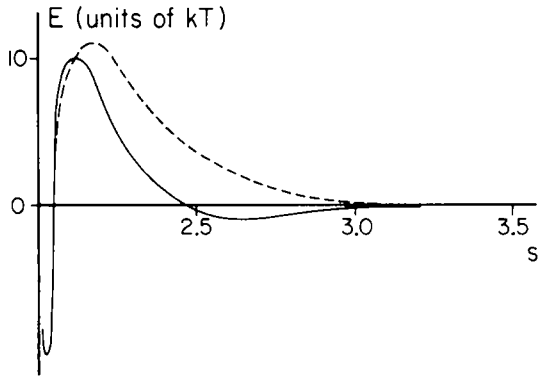

Fig. 7. The total energy of interaction (———) between two identical spheres with radius a and with center-to-center separations R, as a function of the separation parameter $S = R/a$. The curve is drawn to scale from Kruyt (Fig. 24, p. 276) [18]. The dotted line represents a possible shift in the interaction energy curve as a result of the phase change at the pretransition (above T_p).

(nearest surface-to-surface separations of 50—100 Å) associated with the secondary minimum. No conclusive evidence for a purely flocculated state exists. In fact, since the secondary minimum is not very deep unless the particles are large and the energy maximum is low, it is difficult to see how flocculation can occur without coagulation.

The predominant intervesicular interactions forming coagulates are at short distances (nearest surface-to-surface separations of 5—10 Å), at the primary energy minimum. These are strong interactions so a coagulate is not easily disrupted while flocculates are easily dispersed. Since coagulates are larger than individual vesicles, the secondary minimum associated with coagulates is deeper. Under favorable circumstances, coagulated vesicles will flocculate to form aggregates. Aggregates may also arise by coagulation of flocculated vesicles but the means of formation depends on which is the rate-determining process for the particular experimental conditions.

The fused vesicles differ from the initially produced vesicles only by their

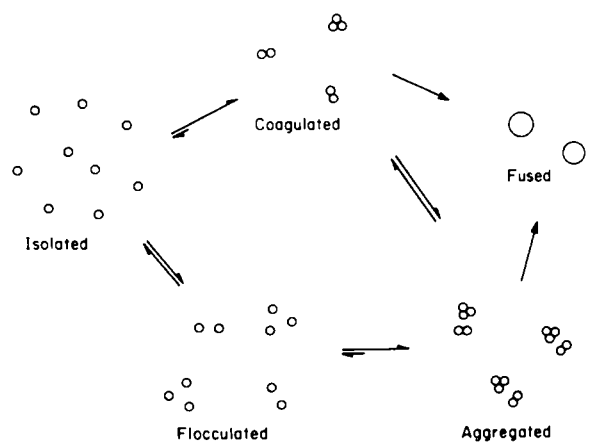

Fig. 8. Schematic representation of possible aggregation states of vesicles in suspension.

size. They can arise only if there is close contact between the vesicle surfaces. Therefore, a prerequisite for fusion is a formation of coagulates or aggregates.

It is well known [21,22] that the light scattering increases when colloidal particles coagulate and flocculate. Consequently, turbidity measurements may be used to monitor the progress of aggregation. In the following we will discuss some of the experimental data which we have reported in this paper in this context.

(i) Vesicles in salt-free solutions. The large absorbance decrease observed at the pretransition while heating these systems (Fig. 3) cannot be accounted for solely by structural changes in the bilayer. Some reversible aggregation phenomenon must contribute to this temperature effect. Since a 10° C temperature rise will not significantly affect the intervesicular interactions, the state of aggregation must also be sensitive to the bilayer phase transition in this temperature range. Coagulates are not easily disrupted by changes in the nature of the colloidal particles, whereas flocculates are very sensitive to surface properties. Therefore, we conclude that it is dispersion of flocculates which contributes to the absorbance decrease at the pretransition.

On cooling, the absorbance increase, and therefore flocculation, follows the time course of the pretransition hysteresis (Figs. 3 and 4). Since flocculation and dispersion are so intimately connected with the pretransition phase change it must introduce a surface potential change. This may result from the altered motional state of the zwitterionic lipid headgroup [23]. An alternative explanation is that intervesicular interactions are sensitive to the presence of facets, which may disappear at temperatures about T_p.

The long term irreversible absorbance increases seen by comparing curves a' and b' in Fig. 3 indicate that a slow coagulation also occurs.

(ii) Vesicles in $Ca(NO_3)_2$ solutions. In $Ca(NO_3)_2$ solutions there is no evidence for vesicle flocculation. The slow decrease in the turbidity ratios shown in Fig. 5B represents coagulation. Since the divalent Ca^{2+} binds to the vesicle surface [9—11], the Stern layer potential [18—20] is altered, abolishing the secondary minimum in Fig. 7, associated with flocculation. Although the surface potential is higher, coagulaton still occurs because of a shielding by the electrolyte double layer formed in the high ionic strength medium. Similar effects are observed with $La(NO_3)_3$ at comparable ionic strength, and are expected for all strongly binding cations.

(iii) Vesicles in monovalent salt solutions. In solutions with NaCl and $NaNO_3$, a combination of the aggregation processes observed in salt-free solutions and with $Ca(NO_3)_2$ is seen. As with no salt, the flocculates disperse readily on heating, but the total absorbance for equivalent dipalmitoyl phosphatidylcholine concentrations is greater at all temperatures, suggesting more coagulation. Because of weak monovalent cation binding the surface potential is not greatly affected. However, the Debye length decreases with electrolyte concentration, enhancing the aggregation.

Finally, we comment on the question of fusion. Studies performed in this laboratory (Lee, Y., Chan, M.K. and Chan, S.I., unpublished observations) show that for phosphatidylcholine samples prepared in $Ca(NO_3)_2$ solution there is no fusion even when they are kept for as long as 14 days at temperatures between 23 and 60° C. These findings support our conclusion that the steady

absorbance change observed in these systems at room temperature is due to coagulation rather than fusion. However, Fig. 6 illustrates that during the first 48 h, cycling through the transition causes a net rise in absorbance (Fig. 6, curves a and b). Fusion has been found in some cases [2,3] to be faster at temperatures around the transition temperature; accordingly we attribute the abrupt absorbance increase in the first heating curves to a fusion process. Presumably, increased coagulation at room temperature predisposes the system to fusion upon heating, and the origin for fusion in these experiments is then the repeated cycling in temperature. The rapid fusion at the thermal transition is interesting, but it remains to be ascertained whether this rapid fusion arises from the presence of boundaries between coexisting liquid-crystalline and gel domains in the bilayer or from the large density fluctuations which are thought to exist under these conditions [24]. However, it was recently demonstrated by Lawaczeck et al. [25] that structural defects generated artificially by low temperature sonication enhanced the rate of fusion even at temperatures well below T_c. These observations point to the importance of lattice defects in the fusion process.

Conclusions

By considering the colloidal nature of vesicle suspensions, we may begin to understand how to control the fusion process. We can ensure that coagulation is rate determining, thereby inhibiting fusion. On the other hand, if coagulation is accelerated, the rate of the fusion process depends on the bilayer stability rather than its surface properties. Certain compounds such as lysophosphatidylcholine could destabilize the bilayer. These concepts are currently being test in this laboratory (Lee, Y.K., Chan, M.K., Eigenberg, K. and Chan, S.I., personal communication).

Acknowledgements

The authors thank Drs. Dov Lichtenberg and Alan E. Blaurock for numerous helpful discussions and Ron Blackman for his technical assistance. This work was supported by Grants GM-14523 and GM-22432 from the National Institute of General Medical Sciences, U.S. Public Health Service.

References

1 Taupin, C. and McConnell, H.M. (1972) Mitochondria/Biomembranes, 9th Fed. Eur. Biochem. Soc. Symp. 28, 219—229
2 Prestegaard, J.H. and Fellmeth, B. (1974) Biochemistry 13, 1122—1126
3 Kantor, H.L. and Prestegaard, J.H. (1975) Biochemistry 14, 1790—1794
4 Papahadjopoulos, D., Hui, S., Vail, W.J. and Poste, G. (1976) Biochim. Biophys. Acta 448, 245—264
5 Lau, A.L. and Chan, S.I. (1974) Biochemistry 13, 4942—4948
6 Tanford, C. (1961) in Physical Chemistry of Macromolecules, Chapter 5, S. Wiley and Sons, Inc., New York
7 Kratochvil, P. (1972) in Light Scattering from Polymer Solutions (Hughlin, H.B., ed.), Chapter 7, Academic Press, London
8 Yi, P.N. and MacDonald, R.C. (1973) Chem. Phys. Lipids 11, 114—134
9 Jacobson, K. and Papahadjopoulos, D. (1975) Biochemistry 14, 152—162
10 Verkleij, A.J., de Kruyff, B., Ververgaert, P.H.J.Th., Tocanne, J.F. and van Deenen, L.L.M. (1974) Biochim. Biophys. Acta 339, 432—437

11 Träuble, H. and Eibl, H. (1974) Proc. Natl. Acad. Sci. U.S. 71, 214—218
12 Tinker, D.O. (1972) Chem. Phys. Lipids 8, 230—257
13 Petersen, N.O. and Chan, S.I. (1977) Biochemistry 16, 2651—2667
14 Ohki, S. and Fukuda, N. (1967) J. Theor. Biol. 15, 362—375
15 Pecora, R. and Aragón, S.R. (1974) Chem. Phys. Lipids 13, 1—10
16 Nagle, J.F. (1973) Proc. Natl. Acad. Sci. U.S. 70, 3443—3444
17 Chong, C.S. and Colbow, K. (1976) Biochim. Biophys. Acta 436, 260—282
18 Kruyt, M.K. (1952) in Colloid Science, Vol. 1, Elsevier Publishing Co., Amsterdam
19 Verwey, E.J.W. and Overbeek, J.Th.G. (1952) in Theory of the Stability of Lyophobic Colloids, Elsevier Publishing Co., Amsterdam
20 Vold, M.J. and Vold, R.D. (1964) in Colloid Chemistry, Van Nostrand Reinhold Co., New York
21 Oster, G. (1947) J. Colloid Sci. 2, 291—299
22 Lips, A. and Willis, E. (1973) Trans. Faraday Soc. 69, 1226—1236
23 McLaughlin, A.C., Cullis, P.R., Berden, J.A. and Richards, R.E. (1975) J. Magn. Reson. 20, 146—165
24 Linden, C.D., Wright, K.L., McConnell, H.M. and Fox, C.F. (1973) Proc. Natl. Acad. Sci. U.S. 70, 2271—2275
25 Lawaczeck, R., Kainosho, M. and Chan, S.I. (1976) Biochim. Biophys. Acta 443, 313—330